1. Cho J, Lee J, Bang H, *et al*. Programmed cell death-ligand 1 expression predicts survival in patients with gastric carcinoma with microsatellite instability. *Oncotarget* 2017; 8: 13320−8.
2. Cancer Genome Atlas Research Network. Comprehensive molecular characterization of gastric adenocarcinoma. *Nature* 2014; 513: 202−9.
3. Cristescu R, Lee J, Nebozhyn M, *et al*. Molecular analysis of gastric cancer identifies subtypes associated with distinct clinical outcomes. *Nat Med* 2015; 21: 449−56.
4. Ma C, Patel K, Singhi AD, *et al*. Programmed death-ligand 1 expression is common in gastric cancer associated with Epstein-Barr virus or microsatellite instability. *Am J Surg Pathol* 2016; 40: 1496−506.
5. An JY, Kim H, Cheong JH, *et al*. Microsatellite instability in sporadic gastric cancer: its prognostic role and guidance for 5-FU based chemotherapy after R0 resection. *Int J Cancer* 2012; 131: 505−11.
6. Min BH, Tae CH, Ahn SM, *et al*. Epstein-Barr virus infection serves as an independent predictor of survival in patients with lymphoepithelioma-like gastric carcinoma. *Gastric Cancer* 2016; 19: 852−9.
7. Muro K, Chung HC, Shankaran V, *et al*. Pembrolizumab for patients with PD-L1-positive advanced gastric cancer (KEYNOTE-012): a multicentre, open-label, phase 1b trial. *Lancet Oncol* 2016; 17: 717−26.
8. Lee J, Kim K-M. Biomarkers for gastric cancer: molecular classification revisited. *Precis Future Med* 2017; 1: 59−68.
9. Mathiak M, Warneke VS, Behrens HM, *et al*. Clinicopathologic characteristics of microsatellite instable gastric carcinomas revisited: urgent need for standardization. *Appl Immunohistochem Mol Morphol* 2017; 25: 12−24.
10. Bae YS, Kim H, Noh SH, *et al*. Usefulness of immunohistochemistry for microsatellite instability screening in gastric cancer. *Gut Liver* 2015; 9: 629−35.
11. Kim ST, Cristescu R, Bass AJ, *et al*. Comprehensive molecular characterization of clinical responses to PD-1 inhibition in metastatic gastric cancer. *Nat Med* 2018; 24: 1449−58.

DOI: https://doi.org/10.1016/j.pathol.2018.09.057

Maternally expressed, paternally imprinted, embryonic non-coding RNA are expressed in osteosarcoma, Ewing sarcoma and spindle cell sarcoma

Sir,

In a human embryo it takes 8 weeks after fertilisation for the skeleton to begin to form, one of the last organs to develop before becoming a foetus. Mesenchymal progenitors, derived from neural crest cells, differentiate into chondrocytes where the skeleton is generated as a mostly cartilage template. Other mesenchymal progenitors envelop the template, activate runt related transcription factor 2 (RUNX2) and bone morphogenetic protein 2 (BMP2) and differentiate into osteoblasts, where an osteoid matrix is secreted and subsequently mineralised to become bone.[1] During development and up to late adolescence, cellular proliferation enabling skeletal growth is restricted to the metaphysis and epiphyseal line or 'growth plate'. It is in the growth plate of long bones where most bone cancers develop, hence the predominantly childhood incidence of the cancer. Primitive mesenchymal cells undergo transformation to form a heterogeneous group of bone malignancies. The most common type of bone cancer in children is osteosarcoma, mostly initiated by tumour protein p53 (*TP53*) structural variants. The second most common type of bone cancer in children is Ewing sarcoma, mostly initiated by a EWS RNA binding protein 1-Fli-1 proto-oncogene, ETS transcription factor (*EWSR1-FLI1*) fusion. There are an average of 160 and 55 new cases of osteosarcoma and Ewing sarcoma, respectively, every year in the UK. Five-year survival for both cancer types is 50% when diagnosed early. Five-year survival is 15% when lung metastases are present at diagnosis. Treatment progress for bone cancer is poor when compared to other cancers such as breast where there is a 20 year survival of 70%. Bone cancer requires extensive and sometimes disabling multimodal treatment. Chemotherapy for osteosarcoma includes methotrexate, cisplatin and doxorubicin, which were developed in the 1940s and 1970s. Chemotherapy for Ewing sarcoma includes vincristine, ifosfamide and etoposide, which were developed in the 1960s and 1980s. If the tumour responds well to chemotherapy and radiotherapy, wide area resection or amputation is performed. New understanding of bone cancer biology leading to better diagnosis and better treatments is required.

Transcriptomic analysis of bone cancer is lacking. Different RNA populations within cells are generally classified as coding and non-coding, i.e., whether they have protein coding potential. Messenger RNA (mRNA) molecules contain a start codon 'AUG' encoding methionine at the beginning of an open reading frame. Non-coding RNA lack protein coding ability and usually exist within the cell without a start codon. Over 70% of known non-coding RNA are long non-coding RNA (lncRNA) that are classed by their >200 nucleotide (nt) length. Similarly to mRNA, lncRNA are transcribed by RNA polymerase II, have a 5′ cap and are polyadenylated. LncRNAs have a large diversity of roles including regulation of chromatin dynamics, enforcing imprinting and as microRNA inhibitors by acting as a microRNA 'sponge'. LncRNAs are further classified based on their genomic localisation. Intergenic lncRNAs are named for their production from loci in between genes. Intronic lncRNAs are named for their production from mRNA introns. Sense lncRNAs are named for their production from the sense strand of protein coding genes that overlap with an exon/intron. Antisense lncRNAs are named for their production from the antisense strand of protein coding genes that overlap with an exon/intron. Another elusive class of non-coding RNA is the small nucleolar RNAs (snoRNAs). SnoRNAs are 60−170 nt in length and are classed as C/D box snoRNAs and H/ACA box snoRNAs. C/D box snoRNAs guide 2′-O-methylation of ribosomal and transfer RNA. H/ACA box snoRNAs guide pseudouridylation mostly in transfer RNAs. The majority of snoRNA are intronic. There is a recent interest in lncRNA and snoRNA and their role in cancer biology. We took a next generation sequencing and bioinformatics approach to evaluate lncRNA and snoRNA expression in bone cancer.

We extracted RNA using the miRCURY RNA isolation kit (Exiqon, Denmark) from two tissue specimens of osteoblastic osteosarcoma (patient ages 15 and 19, OS1 and OS2, respectively). OS1 had undergone treatment with cisplatin and doxorubicin prior to surgery (Fig. 1A,B). OS2 had undergone treatment with methotrexate, cisplatin and doxorubicin prior to surgery (Fig. 1C,D). We extracted RNA from one tissue specimen of Ewing sarcoma (patient age 6, ES) where the patient had undergone nine alternating cycles of vincristine, doxorubicin and cyclophosphamide in one cycle and ifosfamide and etoposide in another cycle prior to surgery (Fig. 1E,F). We extracted RNA from one tissue specimen of a spindle cell sarcoma of bone (patient age 17, SCS) where the patient had not undergone systemic treatment (Fig. 1G,H). We used publicly available data for four control samples, which were obtained from long bone tissue derived from surgical

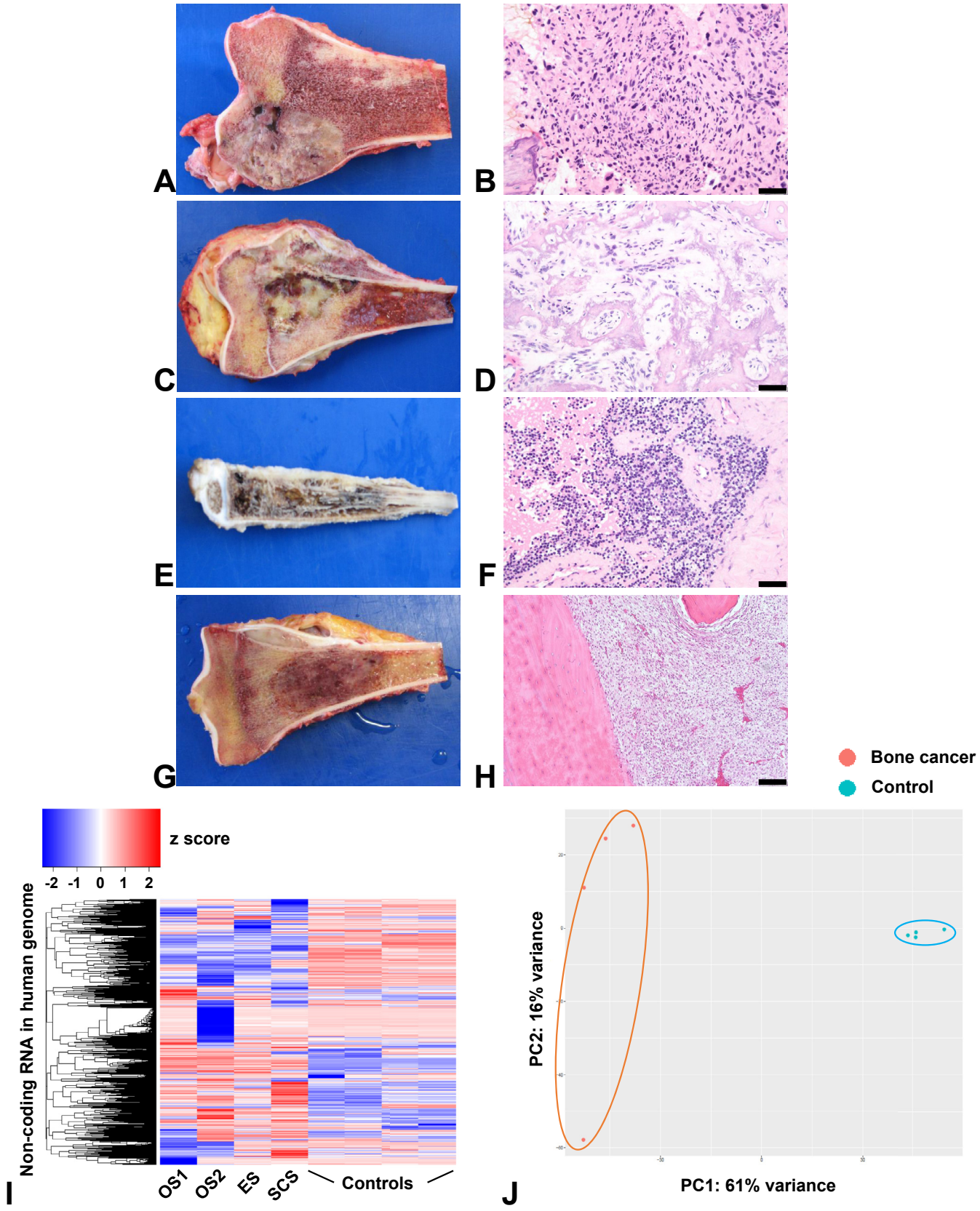

Fig. 1 (A–H) Macroscopic and microscopic photographs of resected tumours used in this study. In the microscopic images, the black scale bar is 100 µM. (A) Osteoblastic osteosarcoma was diagnosed at biopsy. The patient underwent treatment with cisplatin and doxorubicin. On resection, a partly cream/grey focally haemorrhagic tumour was observed. (B) H&E stain of (A) shows a 5% response to chemotherapy (minimal response). Examination is consistent with osteoblastic osteosarcoma. (C) Osteoblastic osteosarcoma was diagnosed at biopsy. The patient underwent treatment with methotrexate, cisplatin and doxorubicin. On resection, a focally gelatinous and haemorrhagic tumour was observed. (D) H&E stain of (C) showed a 95% response to chemotherapy (excellent response). Examination was consistent with osteoblastic osteosarcoma. (E) Ewing sarcoma was diagnosed at biopsy. The patient underwent nine alternating cycles of vincristine, doxorubicin and

Table 1 The 10 most upregulated and 10 most downregulated lncRNA in our bone cancer cohort when compared to control samples, also showing 4 dysregulated snoRNAs

Transcript ID	Human genome annotation	Type	Dysregulation (up/down)	Log_2 fold change
ENST00000617687.1	*AC244100.2-202*	Antisense lncRNA	Up	13.22
ENST00000414790.6	*H19-203*	Intronic lncRNA	Up	12.9
ENST00000535913.2	*SLC12A5-AS1*	Antisense lncRNA	Up	12.69
ENST00000554639.5	*MEG3-224*	Intergenic lncRNA	Up	12.45
ENST00000429829.5	*XIST-204*	Intergenic lncRNA	Up	11.28
ENST00000534150.5	*AP000757.1-201*	Antisense lncRNA	Up	10.97
ENST00000541196.2	*HCP5-204*	Sense lncRNA	Up	10.7
ENST00000404665.3	*TMEM51-AS1*	Antisense lncRNA	Up	10.5
ENST00000416330.1	*XIST-201*	Intergenic lncRNA	Up	10.43
ENST00000618234.4	*AL034397.3-201*	Antisense lncRNA	Up	10.4
ENST00000618925.1	*MALAT1-214*	Intergenic lncRNA	Down	10.85
ENST00000510859.5	*PAX8-AS1-209*	Antisense lncRNA	Down	9.94
ENST00000587245.2	*PRMT5-AS1-203*	Antisense lncRNA	Down	9.88
ENST00000544868.2	*MALAT1-203*	Intergenic lncRNA	Down	9.5
ENST00000637700.1	*MIR100HG-224*	Intergenic lncRNA	Down	9.35
ENST00000468186.5	*THUMPD3-AS1-202*	Antisense lncRNA	Down	9.12
ENST00000412059.5	*GAS5-201*	Intronic lncRNA	Down	7.44
ENST00000620594.1	*ZFAS1-209*	Antisense lncRNA	Down	7.2
ENST00000512932.5	*THAP9-AS1-211*	Antisense lncRNA	Down	6.53
ENST00000534782.3	*MIR100HG-222*	Intergenic lncRNA	Down	6.5
ENST00000363214.1	*SNORD68*	C/D box snoRNA	Up	4.02
ENST00000577988.2	*SNORD3B-1*	C/D box snoRNA	Up	2.86
ENST00000571722.3	*SNORD3B-2*	C/D box snoRNA	Up	2.68
ENST00000607313.1	*SNORD58B*	C/D box snoRNA	Down	2.28

Differentially expressed lncRNA and snoRNA were identified according to $\log_2$ fold change ≥ 2, p value <0.05 and FDR $<5\%$. The full data set is publicly available on GEO under accession GSE113916.

reconstruction procedures (patient ages 11−13).[2] Cancer RNA was stored at −80°C. We generated cDNA libraries using the SENSE mRNA library prep kit (Lexogen, Austria). We performed 150 bp paired end sequencing on the HiSeq 4000 (Illumina, USA).

Raw fastq files were converted to fasta format. Adapter sequences and reads <20 nt were trimmed using Trim Galore (www.bioinformatics.babraham.ac.uk/projects/trim_galore). Trimmed reads were aligned to the human genome (v.38) using HISAT2.[3] The latest set of human non-coding RNAs were downloaded from GENCODE (v.28) and Ensembl (v.92). Count matrix for lncRNAs and snoRNAs was created using Kallisto.[4] LncRNA and snoRNA expression was compared between bone cancer and controls using the DESeq2 package available in R. We selected differentially expressed lncRNA and snoRNA according to $\log_2$ fold change ≥ 2, p value <0.05 and false discovery rate $<5\%$. Hierarchical cluster analysis and principle component analysis investigating 77% of variance showed distinct grouping between cancer and controls (Fig. 1I,J).

We report a *H19* transcript, *H19-203*, is highly expressed in bone cancer (Table 1). *H19* is a maternally expressed, paternally imprinted, embryonic lncRNA.[5] *H19* is a key mediator of sonic hedgehog (*SHH*) signalling in osteoblastic osteosarcoma.[6] SHH ligand is a major embryonic morphogen and is later required for adult stem cell division. *H19* is reciprocally imprinted and regulated with its neighbouring gene insulin like growth factor 2 (*IGF2*).[5] We found a *MEG3* transcript, *MEG3-224*, to have low expression in OS1 and ES (44 reads and 91 reads, respectively, normalised data in GEO). *MEG3-224* expression was high in OS2 and SCS (2091 reads and 1616 reads, respectively, normalised data in GEO) (Table 1). *MEG3* is a maternally expressed, paternally imprinted lncRNA with low expression correlating to poor prognosis in osteosarcoma and other cancers.[7] *XIST-201* and *XIST-204*, products of X inactive specific transcript (*XIST*), were highly expressed in our cohort, with OS1 and ES showing the highest expression (Table 1). *XIST*, located on the X chromosome, has previously been reported as a poor prognostic marker in solid tumours.[8] We also found high expression of *HCP5-204* which has previously been linked to cancer progression via sponging of miR-22, miR-186 and miR-216a.[9] *MALAT1-203* and *MALAT1-214*, products of metastasis associated lung adenocarcinoma transcript 1 (*MALAT1*), were downregulated in this study (Table 1).

We report four dysregulated snoRNAs in our bone cancer samples (Table 1). *SNORD68*, recruited by DExD box helicase 21 (*DDX21*) to enable 2′-O-methylation of residue U428 of the 18S ribosomal RNA (rRNA) sequence, was upregulated in each cancer type (Table 1). *SNORD3B-1* and

cyclophosphamide (cycle 1) and ifosfamide and etoposide (cycle 2). On resection, a lesion with extensive involvement of the medulla and cortex with periosteal elevation was observed. (F) H&E stain of (E) showed a monomorphic population of small round blue cells with hyperchromatic and indistinct nuclei. Cells were positive for CD99 and S100. Cells were negative for CD3, CD20, CD45, CKMNF116, EMA, AE1/3, SMA, desmin and FLI1. *EWSR1* gene rearrangement was observed in 56/72 nuclei. Examination was consistent with Ewing sarcoma. (G) High grade sarcoma was diagnosed at biopsy. On resection, a pale cream/grey and destructive lesion with permeation into underlying bone was observed. (H) H&E stain of (G) showed an infiltrative pattern of growth within the bone and extraosseous extension. Tumour cells were negative for CD30, CD31, CD34, CD45, CD99, CKMNF116, EMA, AE1/3, SMA, desmin, S100, HMB45, STAT6, TLE1, Melan-A, CCNB3 and ALK1. There was no *EWSR1-NR4A3* gene rearrangement. Examination was consistent with spindle cell sarcoma of bone. (I) Heat map based hierarchical cluster analysis of differentially expressed non-coding RNAs (y-axis) between bone cancer, OS1, OS2, ES, SCS and controls (x-axis). Z score refers to high (in red) and low (in blue) non-coding RNA expression using normalised values when compared to the mean of total sequencing reads. (J) A biplot principle component analysis shows two distinct clusters along the PC1 axis that correspond to the bone cancer samples (in orange) and control samples (in blue).

SNORD3B-2, close paralogues of U3 snoRNA, guide site specific cleavage of rRNA during pre-rRNA processing.[10] We report *SNORD3B-1* and *SNORD3B-2* are upregulated in bone cancer (Table 1). *SNORD58B* is reported to guide the 2′-O-methylation of residue G4198 of the 28S rRNA.[11] We found *SNORD58B* was downregulated in our bone cancer samples (Table 1).

RNA therapeutics are on the horizon. LncRNA and snoRNA are of recent interest because of their elusive roles in regulating gene expression and epitranscriptomic modification of pre-RNAs. RNA is also a specific biomarker, which is especially helpful in providing a robust diagnosis in rare and heterogeneous cancers. Bone cancers are historically difficult to diagnose and subclassify prior to surgery, which can delay the appropriate choice of neoadjuvant chemotherapeutic agents. *H19* expression after birth is linked to Beckwith–Wiedemann syndrome, which increases the likelihood of childhood cancer but not adult cancer. We found that *H19-203* may be a specific biomarker for osteosarcomas involving *SHH* signalling. Patients may benefit from receiving targeted *SHH* inhibitors sonidegib or vismodegib that are currently used to treat basal cell carcinoma. We also found low *MEG3-224* and high *XIST-201/XIST-204* may be markers of poor prognosis and lower overall survival in patients, which we detected in two of four patients. Upregulation of snoRNAs is consistent with the increased proliferative behaviour of cancer cells. *SNORD68*, *SNORD3B-1* and *SNORD3B-2* may be useful biomarkers in the future. Previous research has shown the *EWSR1-FLI1* chimaeric transcript in Ewing sarcoma is sensitive to snoRNA loss of function due to changes in splicing, demonstrating a potential target for intervention in Ewing sarcoma cells through snoRNA activity.[12]

A limitation of this study is the size of the cohort studied. Bone cancer is rare and donation to tissue banks is scarce. Our data highlight the value of being able to provide a specific tissue diagnosis in addition to identifying regulatory transcriptomic molecules that could be exploited for targeted therapy.

Acknowledgements: Approval to obtain and study human tissue was granted by the Faculty of Medicine and Health Sciences Research Ethics Committee (2015/16 100 HT). The cancer data presented in this study is publicly available on GEO under the accession GSE113916. The control data used in this study is publicly available on GEO under the accession GSE55282. We thank Lucy Bishton, Natalie Jackson, Dionne Wortley, Kulvinder Jill and Karen Joynes (The Royal Orthopaedic Hospital) for supporting collection of patient samples.

Conflicts of interest and sources of funding: This study was funded by The Humane Research Trust. The authors state that there are no conflicts of interest to disclose.

Darrell Green[1], Archana Singh[2], Jasmine Sanghera[2], Lee Jeys[3], Vaiyapuri Sumathi[4], Tamas Dalmay[2], William D. Fraser[1,5]

[1]Norwich Medical School, University of East Anglia, Norwich Research Park, Norwich, United Kingdom; [2]School of Biological Sciences, University of East Anglia, Norwich Research Park, Norwich, United Kingdom; [3]Department of Orthopaedic Oncology, The Royal Orthopaedic Hospital, Birmingham, United Kingdom; [4]Department of Musculoskeletal Pathology, The Royal Orthopaedic Hospital, Birmingham, United Kingdom; [5]Department of Clinical Biochemistry, Norfolk and Norwich University Hospital, Norwich Research Park, Norwich, United Kingdom

Contact Prof William D. Fraser.
E-mail: W.Fraser@uea.ac.uk

1. Green D, Dalmay T, Fraser WD. Role of miR-140 in embryonic bone development and cancer. *Clin Sci (Lond)* 2015; 129: 863–73.
2. Rojas-Pena ML, Olivares-Navarrete R, Hyzy S, *et al*. Characterization of distinct classes of differential gene expression in osteoblast cultures from non-syndromic craniosynostosis bone. *J Genomics* 2014; 2: 121–30.
3. Pertea M, Kim D, Pertea GM, *et al*. Transcript-level expression analysis of RNA-seq experiments with HISAT, StringTie and Ballgown. *Nat Protoc* 2016; 11: 1650–67.
4. Bray NL, Pimentel H, Melsted P, *et al*. Near-optimal probabilistic RNA-seq quantification. *Nat Biotechnol* 2016; 34: 525–7.
5. Raveh E, Matouk IJ, Gilon M, *et al*. The H19 long non-coding RNA in cancer initiation, progression and metastasis – a proposed unifying theory. *Mol Cancer* 2015; 14: 184.
6. Chan LH, Wang W, Yeung W, *et al*. Hedgehog signaling induces osteosarcoma development through Yap1 and H19 overexpression. *Oncogene* 2014; 33: 4857–66.
7. Tian ZZ, Guo XJ, Zhao YM, *et al*. Decreased expression of long non-coding RNA MEG3 acts as a potential predictor biomarker in progression and poor prognosis of osteosarcoma. *Int J Clin Exp Pathol* 2015; 8: 15138–42.
8. Mao H, Wang K, Feng Y, *et al*. Prognostic role of long non-coding RNA XIST expression in patients with solid tumors: a meta-analysis. *Cancer Cell Int* 2018; 18: 34.
9. Liang L, Xu J, Wang M, *et al*. LncRNA HCP5 promotes follicular thyroid carcinoma progression via miRNAs sponge. *Cell Death Dis* 2018; 9: 372.
10. Clery A, Senty-Segault V, Leclerc F, *et al*. Analysis of sequence and structural features that identify the B/C motif of U3 small nucleolar RNA as the recognition site for the Snu13p-Rrp9p protein pair. *Mol Cell Biol* 2007; 27: 1191–206.
11. Kiss-Laszlo Z, Henry Y, Bachellerie JP, *et al*. Site-specific ribose methylation of preribosomal RNA: a novel function for small nucleolar RNAs. *Cell* 1996; 85: 1077–88.
12. Grohar PJ, Kim S, Rangel Rivera GO, *et al*. Functional genomic screening reveals splicing of the EWS-FLI1 fusion transcript as a vulnerability in Ewing sarcoma. *Cell Rep* 2016; 14: 598–610.

DOI: https://doi.org/10.1016/j.pathol.2018.08.014

Rhabdomyosarcoma with *FUS* re-arrangement: additional case in support of a novel subtype

Sir,

The World Health Organization (WHO) Classification of Bone and Soft Tissue Tumours currently recognises four subcategories of rhabdomyosarcoma, namely, embryonal, alveolar, pleomorphic and spindle cell/sclerosing subtypes.[1] Each is characterised by specific and well-described clinical, morphological and molecular features. Very recently, a novel, rare and molecularly-defined subtype of rhabdomyosarcoma has been identified from RNA sequencing of a series of previously unclassified ‘small round cell sarcomas’.[2] These tumours have in common a highly aggressive biological course, monomorphic epithelioid and spindle cell morphology and the unusual combination of ALK protein over-expression and a defining *FUS* (or *EWSR1*)-*TFCP2* fusion.

In this report, we describe the fifth case of this rare sarcoma and demonstrate for the first time the presence of a large *ALK*